$4f$-derived electronic structure at the surface and in the bulk of α-Ce metal

Yu. Kucherenko,[1] S. L. Molodtsov,[2] M. Heber,[2] and C. Laubschat[2]
[1]*Institute of Metal Physics, National Academy of Sciences of Ukraine, UA-03142 Kiev, Ukraine*
[2]*Institut für Oberflächenphysik und Mikrostrukturphysik, TU Dresden, D-01062 Dresden, Germany*
(Received 18 June 2002; published 25 October 2002)

Resonant photoemission experiments at the $4d \rightarrow 4f$ absorption threshold of α-Ce are reported. Separation of spectral bulk and surface contributions is achieved by quenching the Ce-derived surface emission with a Dy overlayer. As in previous works, the outermost surface layer of α-Ce is found to be γ-like. In contrast to theoretical predictions, however, the "$4f^0$ final-state" signal of the surface is shifted to higher binding energy with respect to α-Ce and γ-Ce bulk emissions. The data are analyzed in the framework of the single-impurity Anderson model. Taking into account the influence of the autoionization channel to resonance process, a larger $4f$ hybridization is concluded than assuming solely a direct photoemission event.

DOI: 10.1103/PhysRevB.66.155116 PACS number(s): 79.60.Bm, 71.28.+d, 73.20.At, 71.20.Eh

I. INTRODUCTION

The γ-α phase transition of Ce metal that is related to a volume collapse by 15% and a loss of magnetic moment at high pressure ($p \geqslant 0.8$ GPa) or low temperatures ($T \leqslant 100$ K) (Ref. 1) has attracted large interest during the last decades.[2] It is by now generally accepted that this phase transition is not due to a simple promotion of the localized $4f$ electron into the valence band but due to hybridization of $4f$ and valence-band states that reduces the $4f$ occupancy only by about 10%. Direct insight into this phenomenon can be obtained from photoemission (PE).[3] $4f$ PE spectra of both α- and γ-Ce reveal a characteristic double-peaked structure, from which one component at around 2 eV binding energy (BE) may be assigned to a $4f^0$ final state expected from the photoionization of a localized $4f^1$ ground-state configuration. The other component appears near the Fermi energy (E_F) indicating a $4f$ configuration close to the one of the ground state. A weak intensity of the latter component in γ-Ce can be taken as indication for an almost localized $4f^1$ ground state in that phase, while a strong increase of this component in α-Ce reflects increasing mixing of $4f$- and valence-band (VB) states. The phenomenon may be quantitatively described in the framework of the single-impurity Anderson model (SIAM).[4–6] From the energy positions and relative intensities of the two spectral components hybridization parameters may be derived that allow a consistent description of the PE spectra and ground-state properties.

The analysis is complicated by the fact, that PE represents a surface-sensitive method and the $4f$-VB hybridization decreases at the surface as a function of atomic coordination.[7–9] Surface and bulk contributions to Ce $4f$ spectra have been discriminated taking advantage of the energy dependence of the mean free path of photoelectrons excited at different photon energies.[8] In fact dehybridization has been observed at the surface leading even in case of α-Ce to a γ-like shape of the surface derived PE spectrum. Unfortunately, the applied method suffers from the reduced spectral resolution at higher photon energies. Additionally, spectral surface contributions are estimated assuming exponential damping of the PE intensity as a function of escape depth and setting the thickness of the outermost atomic surface layer equal to half the lattice constant. These approximations, however, do not consider the atomic structure of the solid and may introduce errors to the data evaluation. As an alternative approach to discriminate bulk and surface emissions the quenching of the latter by deposition of a Dy overlayer has been attempted.[9] Assuming layer-by-layer growth and negligible interdiffusion only the pure Ce $4f$ bulk signal remains after Dy deposition. Then, from the difference to the spectrum of pure Ce metal the shape of the surface emission may be derived. For γ-Ce, surface and bulk components were separated in this way and the surface shift of the $4f^0$ emission was measured for the first time with high-resolution PE.[9] For α-Ce, however, respective experiments are still lacking. Calculations performed on the basis of the SIAM predict for α-Ce a surface shift of the $4f^0$ component to lower BE.[10] If true this is an unique phenomenon since all rare-earth systems known so far reveal surface shifts of the $4f^{n-1}$ final state to higher BE's.[11,12]

In this publication we present high-resolution resonant $4d \rightarrow 4f$ PE data of α-Ce and discriminate bulk and surface contributions by the quenching method. In contrast to the theoretical prediction[10] we find a surface shift of the $4f^0$ peak to higher BE. The data are analyzed in the light of SIAM taking into account a realistic VB density of states (DOS). Good agreement between theory and experiment is achieved. Additionally, the influence of the resonance on the spectral shape is considered. Within the resonance process, hybridized $4d^9 4f^{n+1}$ intermediate states are populated by a dipole transition that decay via autoionization into PE final states. As we will show, not only the intensity but also the shape of the $4f$ PE spectra is influenced by this autoionization channel that complicates the interpretation of PE data.

II. EXPERIMENT

Thin films (150 Å) of α-Ce metal were prepared *in situ* by thermal deposition of high-purity Ce metal onto a W(110) substrate held at a temperature of 50 K during the whole experiment. Stabilization of the correct phase was checked by comparing PE spectra of the present films with those of α-Ce taken from the literature.[3,8] It should be noted that all

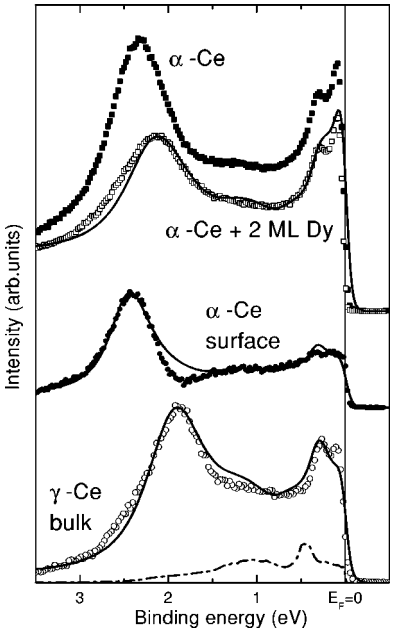

FIG. 1. Experimental resonant PE spectra taken at the Ce $4d \rightarrow 4f$ absorption threshold with 121 eV photon energy: spectrum of clean α-Ce (solid squares) and spectrum of the same sample after deposition of 2 ML Dy (open squares). Surface emission derived from the difference of the spectra of the clean and Dy-covered sample is shown by solid circles. Open circles show a spectrum of bulk γ-Ce obtained by quenching the surface emission by a Dy overlayer (from Ref. 9). Solid lines represent the SIAM simulation of the PE spectra. The VB contribution to the PE spectra is shown with dash-dotted line.

PE spectra found in the literature differ a little from each other due to (i) finite admixtures of β and γ phases in the bulk and (ii) different surface qualities. A large peak at E_F is usually taken as an indication for strong α-like properties. Quenching of the surface Ce emission was achieved by additional deposition of 2 monolayer (ML) Dy metal, which does not contribute to the PE spectra in the energy region of the Ce $4f$ states. Apart from the $4f$ shell, Dy is isoelectronic to γ-Ce and, therefore, no changes of chemical bonding is expected replacing Ce by Dy atoms. On the other hand, the mobility of adsorbed Dy atoms is low at 50 K and interdiffusion may be assumed to be negligible.

PE spectra were taken with a hemispherical VGGLAM2 analyzer exploiting synchrotron radiation from the U-49/2-PGM1 undulator beamline of BESSY II. The basic pressure during the experiments was in the low 10^{-10} mbar range and rose only shortly to 5×10^{-9} mbar during evaporation mainly due to hydrogen emissions. No traces of oxygen and carbon contaminations were found by valence-band PE at 40 eV photon energy.

III. PE SPECTRA AND SURFACE EFFECTS

Figure 1 shows on-resonance valence-band PE spectra of α-Ce, taken at the $4d \rightarrow 4f$ absorption threshold with a spectral resolution of 50 meV. The spectra are dominated by the $4f$ emission, whereas the VB contributions are weak. On-resonance data may be corrected for these contributions by subtracting the off-resonance spectrum that reflects mostly the valence-band DOS because the $4f$ emission is strongly suppressed due to the Fano antiresonance. Although this is the standard procedure, one should note that the VB contributions are underestimated in this way since a part of the VB emission undergoes also a relatively weak resonant enhancement as it has been shown at the $4d \rightarrow 4f$ resonance of La.[13] The VB contribution to the on-resonance emissions, however, remains still small and has no significant effect on the shape of the PE spectrum.

As it can be seen in Fig. 1, the shape of the resonant PE spectrum of α-Ce measured after deposition of 2 ML Dy is substantially changed as compared to that of the pure Ce film. Since the Dy $4f$ states do not contribute in this BE range the PE spectrum reflects pure bulk $4f$ emission of α-Ce.

The surface-derived $4f$ contribution shown by solid circles in Fig. 1 was obtained subtracting the spectrum of Dy covered α-Ce (open squares) from the one of clean α-Ce sample (solid squares). The bulk PE spectrum of γ-Ce taken from Ref. 9 is also presented in the bottom of Fig. 1. Comparing the surface and bulk PE spectra of α-Ce, it is seen, that at the surface (i) the intensity of the low-BE peak (referred to the $4f^1$ final state) is strongly reduced and (ii) the peak appearing in the bulk α-Ce PE spectrum at 2.1 eV BE ($4f^0$ final state) is shifted by 0.3 eV towards larger BE. The relative intensity of the surface-derived $4f^1$ signal with respect to the $4f^0$ emission is even smaller than in the bulk PE spectrum of γ-Ce indicating a weakly hybridized $4f^1$ ground-state configuration.

The observed positive surface energy shift of the $4f^0$ component is in contradiction to the result of Liu *et al.*,[10] who found the $4f^0$ final-state peak in the surface α-Ce PE spectrum shifted to smaller BE with respect to the bulk spectrum. There are, however, two main differences between the work of Liu *et al.* and the present study. First, in Ref. 10 the $4f$ contribution was extracted from PE spectra measured in the photon energy range from 40 to 60 eV taking advantage of the different energy dependence of the $4f$ and $5d$ photoexcitation cross sections, that allowed a discrimination of $4f$ and VB emissions. However, since the respective PE cross sections are of the same order of magnitude in this photon energy range, certain inaccuracy in the determination of the spectral shape of the $4f$ emission are unavoidable. A second, more important difference is that in Ref. 10 the surface and bulk contributions were found as results of a self-consistent fitting of the $4f$ intensity distribution, while in the present work the surface and bulk contributions were separated experimentally.

The analysis of the PE spectra was performed in the framework of SIAM. The variational approach of Gunnarsson and Schönhammer (GS) for the SIAM has been proven to be very successful in interpreting the spectroscopic data.[5] Here we use a rather simple numerical procedure that represents a minimal version of the Gunnarsson-Schönhammer approach and is described in detail in Ref. 6.

Main parameters in the SIAM are the energy of a bare $4f^1$ state denoted as ε_f, the on-site Coulomb repulsion energy

TABLE I. Values of the SIAM parameters and 4f occupancy obtained by fitting the surface and bulk α-Ce PE spectra as well as the bulk γ-Ce PE spectrum (as shown in Fig. 1) considering the PE process as a direct 4f photoexcitation.

Spectrum	ε_f(eV)	Δ(eV)	n_f
bulk α-Ce	−1.45	0.82	0.976
surface α-Ce	−1.89	0.79	1.008
bulk γ-Ce	−1.45	0.68	0.998

U_{ff}, as well as the hybridization strength Δ describing the interaction of the 4f state with the VB via hopping. We chose $U_{ff}=7.5$ eV, the 4f spin-orbit splitting was taken equal to 0.3 eV, whereas the two other parameters ε_f and Δ were found by fitting the experimental curves in order to reproduce the energy separation of the f^0 and f^1 final-state peaks and their intensity ratio. A VB component contributing by 14% of the total integral PE intensity was also taken into account considering the fact that the total PE intensity of Ce varies by about a factor of 20 when going from off to on resonance, while the respective resonant variation of the VB intensity of La amounts only to about 3.[13] The shape of the VB component was taken from the valence-band DOS for Ce metal calculated by means of an optimized method of linear combination of atomic orbitals (LCAO)(Ref. 14) in its scalar relativistic version.[15] We used an energy-dependent lifetime broadening parameter in the form $\Gamma_L(E)=0.03$ eV $+0.085E$ where E denotes the BE with respect to E_F. To take into account instrumental resolution all calculated spectra were additionally broadened with a Gaussian ($\Gamma_G=0.05$ eV). As it can be seen in Fig. 1, the SIAM calculations give a good description of the shape of the experimental spectra. Note, that the small deviations between the bulk spectra of α- and γ-Ce and the results of the respective SIAM simulation at the high-BE side of the $4f^0$ final-state signal may be caused by emissions from residual Ce atoms at the surface of the Dy covered samples. The difference between theory and experiment at the low-BE side of the surface-derived 4f peak may be attributed to changes of the DOS at the surface as discussed below.

The obtained values of the SIAM parameters are summarized in Table I. For bulk γ-Ce the same value of ε_f is found as for bulk α-Ce, whereas the hybridization parameter Δ is strongly decreased. This is a result of larger interatomic distances in γ-Ce leading to weaker 4f-VB hybridization. Consequently, the 4f occupancy becomes very close to 1. At the surface of α-Ce that is also characterized by a weakened hybridization as compared to bulk α-Ce, we find quite different situation. The value of Δ is decreased only by about 5%, whereas ε_f is significantly shifted towards higher BE. This corresponds to the surface core-level shift predicted to be 0.3 eV for close-packed surfaces of γ-Ce.[12] Considering the fact that for metal films deposited at low temperatures the surface shift increases by about 50% due to the presence of low-coordinated surface sites[16] the obtained increase of $|\varepsilon_f|$ by 0.44 eV is in good agreement with the expectation. The relatively weak variation of Δ with respect to its bulk value is somewhat surprising since a proportionality to the change of coordination is expected. This relatively large value of Δ might be taken as an indication for changes of the DOS at the surface, particularly a larger DOS at E_F due to, e.g., surface states.[9,11] In spite of the large Δ, the increased value of $|\varepsilon_f|$ leads to a 4f occupancy close to 1.

IV. EFFECT OF THE AUTOIONIZATION CHANNEL

In the theoretical simulations of the resonant PE spectra the autoionization channel was usually not taken properly into account, in spite it may lead to the f^n final-state configuration weights that are different from those of the direct PE channel, as it was shown by the model calculations in Ref. 17. This was also confirmed by interpretation of the experimental resonant PE data on Ce 3d core-level spectra[18] as well as Ce constant-initial-state spectra[18,19] of Ce compounds.

In the following the reader is referred to Ref. 6 what concerns the basic theoretical model. Here we show, how this model can be extended to describe the resonant PE spectra.

With the ground state $|g\rangle$ (the ground-state energy is E_g) and the final states $|m\rangle$ (their energies are $E_{\rm fin}^{(m)}$) the f spectral weight can be written as [see the formula (22) of Ref. 6]

$$I_f(\epsilon_{\rm kin})=-\frac{1}{\pi}{\rm Im}\sum_m \frac{|\langle m|T|g\rangle|^2}{\hbar\omega-\epsilon_{kin}-(E_{\rm fin}^{(m)}-E_g)+i\Gamma}, \quad (1)$$

where the sum is taken over all final states of the system. The transition operator T for 4f photoexcitation has been written in the matrix element as (f_ν is the annihilation operator for a f electron in the state ν)

$$T=t_f(\omega)f_\nu. \quad (2)$$

The specific form of T dependence on the photon energy $\hbar\omega$ was not given explicitly in Ref. 6. If only the direct PE channel is considered, i.e., the process

$$4d^{10}4f^n(5d6s)^3\rightarrow 4d^{10}4f^{n-1}(5d6s)^3+e^-, \quad (3)$$

t_f is a dipole transition matrix element. For the photoelectron kinetic energies above 100 eV it changes its value only slightly if the energy varies by several electron volts, and this energy dependence could be neglected.

Now, in order to consider the autoionization channel

$$4d^{10}4f^n(5d6s)^3\rightarrow 4d^9 4f^{n+1}(5d6s)^3 \rightarrow 4d^{10}4f^{n-1}(5d6s)^3+e^-, \quad (4)$$

we have to define an intermediate state $|r\rangle$ with a core hole and an additional 4f electron. We introduce also t_c, a dipole transition matrix element for core-level excitation, and v_A, transition matrix element for 4d-4f-4f Auger decay of the intermediate state. Then, the transition operator may be written as

$$T = t_f f_\nu + \sum_r v_A \sum_{\nu'} c^+_{\nu'} f_{\nu'} f_\nu \times \frac{|r\rangle\langle r|}{\hbar\omega - (E^{(r)}_{int} - E^{(1)}) + i\Gamma_{int}} t_c f^+_{\nu'} c_{\nu'}, \quad (5)$$

where the first term corresponds to the direct PE whereas the second term describes the autoionization. The dependence of T on the photon energy $\hbar\omega$ gives rise to the Fano-resonance behavior of the PE signal. Here, $c^+_{\nu'}$ ($c_{\nu'}$) are creation (annihilation) operators for a core electron, $E^{(r)}_{\rm int}$ is the energy of the intermediate state $|r\rangle$, whereas $\Gamma_{\rm int}$ depends, in general, on the $4f$ configuration of the intermediate state and describes its spectral broadening. The expression (5) follows from lowest-order time-dependent perturbation theory and is a simplified version of the formulas (3.21), (3.22) of Ref. 17, where a general theory of resonant PE in the framework of the treatment by Gunnarsson and Schönhammer[5] was given.

To perform the calculations we introduce basis functions for the intermediate states

$$|1\rangle_c = \frac{1}{\sqrt{N_f}} \sum_\nu f^+_\nu c_\nu |\Psi\rangle,$$

$$|2;i\rangle_c = \frac{1}{N_f} \sum_{\nu\nu'}^{\nu\neq\nu'} f^+_\nu f^+_{\nu'} d_{i\nu'} c_\nu |\Psi\rangle,$$

$$|3;ii\rangle_c = \frac{1}{\sqrt{2}} \frac{1}{N_f\sqrt{N_f}} \sum_{\nu\nu'\nu''}^{\nu\neq\nu'\neq\nu''} f^+_\nu f^+_{\nu'} f^+_{\nu''} d_{i\nu''} d_{i\nu'} c_\nu |\Psi\rangle,$$

$$|3;ij\rangle_c = \frac{1}{N_f\sqrt{N_f}} \sum_{\nu\nu'\nu''}^{\nu\neq\nu'\neq\nu''} f^+_\nu f^+_{\nu'} f^+_{\nu''} d_{i\nu''} d_{j\nu'} c_\nu |\Psi\rangle \quad (i>j). \quad (6)$$

These basis functions are consistent with the ground-state basis functions[6] and describe f^1, f^2, and f^3 configurations in the presence of a core hole. Taking the basis functions (6) we obtain a Hamiltonian matrix that differs from the ground-state matrix [formula (15) of Ref. 6] by additional terms $\varepsilon_f - U_{fc} + (n-1)U_{ff}$ in the diagonal matrix elements. Here U_{fc} is the core-hole Coulomb interaction energy, and n is the number of f electrons in the corresponding intermediate-state configuration. Diagonalizing the Hamiltonian matrix, we obtain the eigenenergies $E^{(r)}_{int}$ as well as expansion coefficients for the eigenfunctions $|r\rangle$ of the intermediate states.

We performed the calculations using the transition operator (5) and solving the eigenvalue problem for the intermediate states as described above. The effect of the core hole was described by an attractive energy $U_{fc}=9.77$ eV in agreement with values applied in the literature.[10] In order to characterize the relative weights of the direct and autoionization PE channels we introduced a ratio $\tau = v_A t_c / t_f$, so that $\tau=0$ corresponds to direct photoexcitation, and increasing values of τ mean increasing amplitude of the autoionization channel. The parameter $\Gamma_{\rm int}$ was chosen to be equal to 0.25 eV. Fitting the bulk α-Ce PE spectrum with different values of τ (all taken at the energy of the resonance maximum) gives the SIAM parameters presented in Table II. It can be seen, that inclusion of the autoionization channel in the theoretical model influences considerably the values of the SIAM parameters obtained by fitting the simulated curve to the experimental data. An increased amplitude of the autoionization channel causes a shift of ε_f to lower BE and an increase of Δ. This is due to the fact, that "$4f^0$" and "$4f^1$" features resonate at slightly different energies.[17–19] At the $\hbar\omega=121$ eV resonance maximum the $4f^1/4f^0$ intensity ratio is, therefore, decreased with respect to its value expected for a direct PE process. In order to compensate this effect in the fitting procedure, larger Δ and smaller $|\varepsilon_f|$ values are necessary and, consequently, smaller n_f values are concluded. Additionally, larger Δ values will increase the $4f_{5/2}/4f_{7/2}$ intensity ratio of the Fermi peak leading to a better agreement between theory and experiment in this binding-energy region.

TABLE II. Values of the SIAM parameters, $4f$ occupancy and integral resonance intensity obtained by fitting the bulk α-Ce PE spectrum for different transition matrix element ratios τ.

τ	ε_f(eV)	Δ(eV)	n_f	$I_{\rm tot}/I_{\rm dir}$
0.0	−1.45	0.820	0.976	1.0
0.2	−1.40	0.833	0.962	1.66
0.4	−1.36	0.845	0.947	2.87
0.6	−1.34	0.853	0.937	4.69
0.8	−1.32	0.860	0.927	7.09
1.0	−1.31	0.865	0.921	10.14
1.2	−1.30	0.866	0.918	13.95
1.4	−1.30	0.866	0.918	18.58

For $\tau>1$ the autoionization channel enhances the integral spectral intensity by more than a factor of 10 and dominates in the PE process. In this case the SIAM parameters reach the values that are characteristic for the pure autoionization channel and show no further changes at larger values of τ. It can be seen from Table III, that although taking into account the influence of the autoionization channel to the resonance process changes the estimated values of the SIAM parameters, all conclusions drawn in Sec. III on their behavior when going from α-like to γ-like systems remain valid. Note, that the effect of the autoionization is more pronounced for a strongly hybridized system, namely for the bulk of α-Ce.

TABLE III. Values of the SIAM parameters and $4f$ occupancy obtained by fitting the surface and bulk α-Ce PE spectra as well as the bulk γ-Ce PE spectrum (as shown in Fig. 1) considering the autoionization channel as dominating one in the PE process ($\tau=1.4$).

Spectrum	ε_f(eV)	Δ(eV)	n_f
bulk α-Ce	−1.30	0.866	0.918
surface α-Ce	−1.82	0.832	1.003
bulk γ-Ce	−1.36	0.720	0.994

In order to estimate the values of the SIAM parameters in the framework of the model that includes the resonance process, one needs the values of the transition matrix elements t_f, t_c, and v_A. An accurate theoretical description of the resonant PE spectra can be achieved, if the resonant enhancement of the VB contribution (i.e., $4d$-$4f$-$5d$ Auger decay of the intermediate states) is also taken into account. The corresponding investigations are now in progress.

V. CONCLUSIONS

Separation of bulk and surface contributions to the $4f$-derived resonant PE spectra of α-Ce by means of the quenching overlayer shows, that the surface signal differs from the bulk spectrum by a strongly decreased intensity of the Fermi-level feature and a shift of the $4f^0$-final-state peak by about 0.3 eV towards higher BE. The latter observation is in sharp contrast to previous results, where a surface shift towards lower BE was concluded.

The analysis of the experimental PE spectra in the framework of SIAM shows that a weakened hybridization at the surface of α-Ce is caused mainly by a strong surface shift of ε_f. On the contrary, for the bulk of γ-Ce ε_f has the same value as for the bulk of α-Ce, and the $4f$-VB hybridization is decreased due to a reduced value of Δ.

Taking into account the autoionization in the theoretical model may considerably change the values of the SIAM parameters. For an accurate quantitative interpretation of the resonant PE spectra it is necessary to know the values of transition matrix elements or, at least, the relative weights of the direct and autoionization PE channels.

ACKNOWLEDGMENTS

This work was supported by the Deutsche Forschungsgemeinschaft, SFB 463, Projects Nos. B2, B4, and B11. Expert assistance by the staff of BESSY is acknowledged.

[1] K.A. Gschneidner, Jr., R.O. Elliott, and R.R. McDonald, J. Phys. Chem. Solids **23**, 1191 (1962); D.C. Koskimaki and K.A. Gschneidner, Jr., Phys. Rev. B **11**, 4463 (1975).

[2] R. Ramirez and L.M. Falicov, Phys. Rev. B **3**, 2425 (1971); W.E. Pickett, A.J. Freeman, and D.D. Koelling, *ibid.* **23**, 1266 (1981); J.W. Allen and L.Z. Liu, *ibid.* **46**, 5047 (1992); Z. Szotek, W.M. Temmerman, and H. Winter, Phys. Rev. Lett. **72**, 1244 (1994); B. Johansson, I.A. Abrikosov, M. Aldén, A.V. Ruban, and H.L. Skriver, *ibid.* **74**, 2335 (1995); J.W. van der Eb, A.B. Kuzmenko, and D. van der Marel, *ibid.* **86**, 3407 (2001); M.B. Zölfl, I.A. Nekrasov, Th. Pruschke, V.I. Anisimov, and J. Keller, *ibid.* **87**, 276403 (2001); K. Held, A.K. McMahan, and R.T. Scalettar, *ibid.* **87**, 276404 (2001).

[3] D. Wieliczka, J.H. Weaver, D.W. Lynch, and C.G. Olson, Phys. Rev. B **26**, 7056 (1982); E. Wuilloud, H.R. Moser, W.-D. Schneider, and Y. Baer, *ibid.* **28**, 7354 (1983); A. Fujimori and J.H. Weaver, *ibid.* **32**, 3422 (1985); F. Patthey, B. Delley, W.-D. Schneider, and Y. Baer, Phys. Rev. Lett. **55**, 1518 (1985).

[4] P.W. Anderson, Phys. Rev. **124**, 41 (1961).

[5] O. Gunnarsson and K. Schönhammer, Phys. Rev. Lett. **50**, 604 (1983); Phys. Rev. B **28**, 4315 (1983); J.W. Allen, S.-J. Oh, O. Gunnarsson, K. Schönhammer, M.B. Maple, M.S. Torikachvili, and I. Lindau, Adv. Phys. **35**, 275 (1986).

[6] R. Hayn, Yu. Kucherenko, J.J. Hinarejos, S.L. Molodtsov, and C. Laubschat, Phys. Rev. B **64**, 115106 (2001).

[7] C. Laubschat, E. Weschke, C. Holtz, M. Domke, O. Strebel, and G. Kaindl, Phys. Rev. Lett. **65**, 1639 (1990); O. Eriksson, R.C. Albers, A.M. Boring, G.W. Fernando, Y.G. Hao, and B.R. Cooper, Phys. Rev. B **43**, 3137 (1991); Y. Baer, M. Grioni, D. Malterre, and W.-D. Schneider, *ibid.* **44**, 9108 (1991); D.L. Price, *ibid.* **60**, 10 588 (1999).

[8] E. Weschke, C. Laubschat, T. Simmons, M. Domke, O. Strebel, and G. Kaindl, Phys. Rev. B **44**, 8304 (1991).

[9] E. Weschke, A. Höhr, G. Kaindl, S.L. Molodtsov, S. Danzenbächer, M. Richter, and C. Laubschat, Phys. Rev. B **58**, 3682 (1998).

[10] L.Z. Liu, J.W. Allen, O. Gunnarsson, N.E. Christensen, and O.K. Andersen, Phys. Rev. B **45**, 8934 (1992).

[11] G. Kaindl, A. Höhr, E. Weschke, S. Vandré, C. Schüßler-Langeheine, and C. Laubschat, Phys. Rev. B **51**, 7920 (1995).

[12] M. Aldén, B. Johansson, and H.L. Skriver, Phys. Rev. B **51**, 5386 (1995).

[13] C.G. Olson, P.J. Benning, M. Schmidt, D.W. Lynch, P. Canfield, and D.M. Wieliczka, Phys. Rev. Lett. **76**, 4265 (1996); S.L. Molodtsov, M. Richter, S. Danzenbächer, S. Wieling, L. Steinbeck, and C. Laubschat, *ibid.* **78**, 142 (1997).

[14] H. Eschrig, *Optimized LCAO Method* (Springer, Berlin, 1989).

[15] M. Richter and H. Eschrig, Solid State Commun. **53**, 529 (1989).

[16] W.-D. Schneider, C. Laubschat, and B. Reihl, Phys. Rev. B **27**, 6538 (1983).

[17] O. Gunnarsson and T.C. Li, Phys. Rev. B **36**, 9488 (1987).

[18] H. Ogasawara, A. Kotani, P. Le Fevre, D. Chandesris, and H. Magnan, Phys. Rev. B **62**, 7970 (2000).

[19] L. Braicovich, C. Carbone, O. Gunnarsson, and G.L. Olcese, Phys. Rev. B **44**, 13 756 (1991).